Asp^{433} in the closing gate of ASIC1 determines stability of the open state without changing properties of the selectivity filter or Ca^{2+} block

Tianbo Li, Youshan Yang, and Cecilia M. Canessa

Department of Cellular and Molecular Physiology, Yale University, New Haven, CT 06520

A constriction formed by the crossing of the second transmembrane domains of ASIC1, residues G432 to G436, forms the narrowest segment of the pore in the crystal structure of chicken ASIC1, presumably in the desensitized state, suggesting that it constitutes the "desensitization gate" and the "selectivity filter." Residues Gly-432 and Asp-433 occlude the pore, preventing the passage of ions from the extracellular side. Here, we examined the role of Asp-433 and Gly-432 in channel kinetics, ion selectivity, conductance, and Ca^{2+} block in lamprey ASIC1 that is a channel with little intrinsic desensitization in the pH range of maximal activity, pH 7.0. The results show that the duration of open times depends on residue 433, with Asp supporting the longest openings followed by Glu, Gln, or Asn, whereas other residues keep the channel closed. This is consistent with residue Asp-433 forming the pore's closing gate and the properties of the side chain either stabilizing (hydrophobic amino acids) or destabilizing (Asp) the gate. The data also show residue 432 influencing the duration of openings, but here only Gly and Ala support long openings, whereas all other residues keep channels closed. The negative charge of Asp-433 was not required for block of the open pore by Ca^{2+} or for determining ion selectivity and unitary conductance. We conclude that the conserved residue Asp-433 forms the closing gate of the pore and thereby determines the duration of individual openings while desensitization, defined as the permanent closure of all or a fraction of channels by the continual presence of H^+, modulates the on or off position of the closing gate. The latter effect depends on less conserved regions of the channel, such as TM1 and the extracellular domain. The constriction made by Asp-433 and Gly-432 does not select for ions in the open conformation, implying that the closing gate and selectivity filter are separate structural elements in the ion pathway of ASIC1. The results also predict a significantly different conformation of TM2 in the open state that relieves the constriction made by TM2, allowing the passage of ions unimpeded by the side chain of Asp-433.

The Journal of General Physiology

INTRODUCTION

The second transmembrane segment (TM2) lines most of the ion pathway of the acid-sensing ion channels (ASICs) and of all other members of the ENaC/degenerin family of ion channels. The functional contributions of residues in TM2 have been difficult to explore, partly because of low tolerance to mutagenesis. Substitutions of most residues in TM2 either markedly decrease or completely abolish currents, consistent with TM2 playing essential roles in permeation and gating of the channel. The functional importance of TM2 is also reflected by a very high amino acid conservation of this segment among all ASICs, despite variations in gating properties and to a lesser extent in ion selectivity among all ASIC channels examined to date.

Asp-433 in TM2 is of particular interest because the carboxylic group occludes the pore in the external side of a constriction that defines the narrowest point in the permeation pathway according to the atomic structure of chicken ASIC1 solved by Gonzales et al. (2009). The constriction, referred to as "desensitization gate," is formed by the crossing of TM2s from each of the three subunits and extends ~8 Å from Gly-432 to Gly-436. Gly-432 is the site of the degenerin mutations, which produce a component of constitutive open channels at baseline pH 7.4, leading to neuronal death in *Caenorhabditis elegans* (Chalfie and Wolinsky, 1990; Driscoll and Chalfie, 1991).

Besides forming the putative desensitization gate, these residues may also play a role in defining ion selectivity, as suggested by the carbonyl oxygen of Gly-432 together with the carboxylic oxygen of Asp-433 coordinating a Cs^+ ion at the entrance of the pore in the atomic structure of cASIC1. Previous work also showed that Ca^{2+} ions reduce the unitary currents by producing fast block of rat ASIC1a in the open state (de Weille and Bassilana, 2001; Zhang and Canessa, 2002; Immke and McCleskey, 2003), and furthermore that Ca^{2+} probably binds Asp-433 to mediate those observations (Paukert et al., 2004).

To explore the role of Asp-433 and Gly-432 in the functional properties of ASIC1, we examined the effects of these residues in the kinetics of lamprey ASIC1,

Correspondence to Cecilia M. Canessa: cecilia.canessa@yale.edu

Abbreviations used in this paper: ASIC, acid-sensing ion channel; TEVC, two-electrode voltage clamp recording.

The Rockefeller University Press $30.00
J. Gen. Physiol. Vol. 137 No. 3 289–297
www.jgp.org/cgi/doi/10.1085/jgp.201010576

which is a channel with little proton-induced desensitization in the pH range of 7.4–6.8, despite having identical residues in the putative desensitization gate (Li et al., 2010). More importantly, we used lASIC1 because this channel tolerates mutations that render rat and chicken ASIC1a inactive, thereby markedly limiting analysis to the residues of interest. We found that substitutions of Asp-433 and Gly-432 change the duration of the open events, consistent with these residues modulating the closing of the pore. In contrast, the selectivity of permeant ions and the magnitude of the unitary conductance were not changed, implying that a different structure in TM2 makes up the selectivity filter of ASIC1. Finally, we found that fast Ca^{2+} block of the open pore does not require a negative charge in position 433, as the Ca^{2+} affinity and voltage dependence of block were not changed by the mutant D433Q, thereby suggesting that Asp-433 is most likely protonated in the open state.

MATERIALS AND METHODS

Molecular biology

Point mutations in the cDNA of lamprey ASIC1-FLAG in pCR2.1 vector were introduced using QuickChange (Agilent Technologies). All products were sequenced to confirm the presence of the mutations. cDNAs were linearized with HindIII restriction enzyme and transcribed in vitro using the T7 mMESSAGEmMACHINE kit (Applied Biosystems). *Xenopus laevis* oocytes were injected with 1–20 ng cRNA in a volume of 50 nl. Electrophysiological studies were conducted 2–3 d after injection. Oocytes were prepared by standard procedures (Zhang et al., 2006) from frog ovaries purchased from Nasco.

Biotinylation of proteins and Western blotting

Eight oocytes per condition were biotinylated with sulfo-NHS-SS-Biotin (Thermo Fisher Scientific) on ice. After lysis of cells with 1% Triton X-100 and centrifugation at 8,000 *g* for removal of the yolk, biotinylated proteins were recovered with streptavidin beads (Thermo Fisher Scientific). The beads were washed with 1% Triton X-100 and 300 mM NaCl. Biotinylated proteins were eluted from beads, resolved in 10% SDS-PAGE, and transferred to PVDF membranes (Millipore). lASIC1 was detected with horseradish peroxidase–conjugated anti-FLAG monoclonal antibody (Sigma-Aldrich). Signals were developed with ECL+ (GE Healthcare) and exposed to BioMax MR film (Kodak).

Two-electrode voltage clamp recordings (TEVCs)

TEVCs of oocytes were done using the Clamp OC-725B amplifier (Warner Instruments). Data were digitized at a sampling rate of 2 kHz (PowerLab 4/30; ADInstruments). Oocytes were placed in a recording chamber (400 µl) perfused by gravity at a rate of 4 ml/min and impaled with two glass microelectrodes filled with 3 M KCl, with a resistance <1 MΩ. Composition of the standard bath solution (in mM): 120 NaCl, 2 KCl, 1.5 $CaCl_2$, and 20 HEPES, with pH >6.5 of 20 mM MES for pH ≤6.5. Apparent proton affinities were calculated with:

$$I = 1/(1+(EC_{50}/[H^+])^n). \quad (1)$$

Patch clamp recordings

Patch clamp recordings were conducted in the outside-out configuration. Patch pipettes were pulled from PG150T glass (Warner Instruments) to tip diameter of 2–4 µm after heat polishing. Pipette solution was (in mM): 120 KCl, 5 EDTA, and 20 HEPES titrated with KOH to pH 7.4. Bath and activating solutions were the same as in TEVC experiments. Activating solutions were applied using a modified Perfusion Fast Step device (SF-77B; Warner Instruments) onto which eight perfusion pipettes were mounted. A data acquisition program (Pulse; HEKA) controlled the SF-77B. Recordings were made using an amplifier (EPC-9; HEKA) and the Pulse acquisition program. Membrane potential was held at −60 mV. Experiments were conducted at room temperature.

Relative permeabilities to monovalent cations

Currents were measured at various voltages from −100 to 20 mV in 10-mV steps while the bathing solution contained 120 mM of single monovalent cations: Na^+, Li^+, K^+, or Cs^+ buffered at pH 6.8. Relative permeabilities were calculated according to:

$$\Delta E_{rev} = E_{revB} - E_{revA} = \frac{RT}{zF}\ln\frac{P_B[B]_o}{P_A[A]_o}, \quad (2)$$

where E_{revA} indicates the reversal potential for Na^+, RT/zF has the usual meaning, and $[B]_o$ is the concentration of the ion in the external bath, 120 mM (Hille, 1992).

Voltage dependence of Ca^{2+} block

The voltage dependence of Ca^{2+} block was calculated with the Boltzmann equation:

$$K_D(V) = K_D(0)e^{(z\delta FV/RT)}, \quad (3)$$

where $K_D(0)$ is the value of K_D at 0 mV, z is the charge valence of blocking ion, δ is the fraction of the electric field that the blocker traverses to reach the site, F is the Faraday's constant, R is the gas constant, and T is absolute temperature (Woodhull, 1973).

Histograms of mean open times

Patch clamp records containing one or two simultaneous opening events were idealized, and the duration of each opening was tabulated manually using a 50% amplitude threshold. The values were grouped in bins, and histograms were generated using Excel software (Microsoft). The data were fitted with two or three exponential functions using the least-square best-fit routine of KaleidaGraph software (Synergy Software).

RESULTS

Substitutions of Gly-432 and Asp-433 change the magnitude of the macroscopic currents

The five residues in TM2 that form the constriction at the entrance of the pore, Gly-432 to Gly-436, are conserved in all ASICs cloned to date, despite differences in speed and extend of desensitization among these channels. Lamprey ASIC1 is an example of a channel exhibiting little desensitization (Li et al., 2010). To explore whether and how replacement of Gly-432 or Asp-433 changes the kinetics of lASIC1, we introduced the mutations shown in Fig. 1 (A and C) and measured the maximal current induced by pH 6.0. Data were normalized to the mean value of channels bearing Gly-432 (14.5 ± 2.3 µA/cell) and Asp-433 (16.3 ± 4.1 µA/cell), respectively. Each column represents the average ± SD of at least 12 cells obtained from three different oocyte preparations.

Cys and Ala in position 432 were functional with 30% higher currents than wild type, but other residues with larger side chains completely eliminated currents. Mutants that did not respond to pH 6.0 were exposed to lower pH, in the range of <6.0 to 5.0, but in no case did stronger stimuli evoke currents, indicating that the absence of response could not be simply attributed to a displacement of the apparent proton affinity for activation (pH_{50A}).

Decreased level of protein expression or defective traffic to the plasma membrane was also not an explanation, as all mutants expressed robustly at the cell surface examined by biotinylation and Western blot analysis of channels on the plasma membrane (Fig. 1, B and D). To boost current expression, some oocytes received a 10-fold larger amount of cRNA, mutants D433N and D433G, which led to a two- to threefold increased level of protein expression but did not improve functional expression. Hence, we conclude that most of the substitutions severely impaired activation or forced channels to remain in a shut conformation. There was a nonlinear relation between the amount of cRNA injected and the steady-state level of protein, most likely a result of the saturation of synthesis/processing of channels injected with large amounts of cRNA.

The same substitutions of Gly-432 and Asp-433 introduced in rat ASIC1 produced nonfunctional channels or led to current levels that were too small for further analysis (≤0.22 μA/cell).

Channels bearing substitutions of Asp-433 exhibit partial desensitization

The time course of macroscopic currents of lASIC1 with substitutions of Asp-433 exhibits various degrees of partial desensitization in contrast to the sustained currents of wild-type channels. Fig. 2 shows biphasic decay in the continual presence of pH 6.5: the initial peak is followed by a steady component. Returning the pH to 7.6 brings the currents to the zero level. Fig. 2 also shows the time course of the macroscopic current of the mutants G432C and G432A that exhibit only non-desensitizing currents similar to the parent channel. However, the mutations increased the magnitude of the currents, as shown in Fig. 1 A. We will show later that this is the result of lengthening the duration of mean open times.

Polar residues Gln and Asn in position 433 shorten the duration of openings

We next examined single-channel kinetics of channels bearing substitutions of Asp-433. Fig. 3 A shows current traces of excised patches in the outside-out configuration containing ∼200 wild-type channels (WT:D433) activated by pH 7.1 and 6.9. Fig. 3 B illustrates current traces with single-channel events. The first trace contains an opening that lasts 10 s, the whole duration of the sweep. The second and third traces show in addition shorter openings marked by a stippled line above the current. From eight successful patches containing a single channel, we recorded 2,802 events. The low number of events was a result of some sweeps having only one or two very long openings. A histogram of open events is shown in Fig. 3 C, where the line is the fit with three exponential components. Open events could be divided into three categories: short duration, <10 ms (51%); intermediate duration, 10–100 ms (35.5%); and long duration, 1,000 ms (13%), including some lasting >10 s.

The mutants D433Q and D433N exhibit markedly different kinetics from wild-type channels. The duration of openings was reduced, and some openings were grouped in long successions of brief open and shut events that produced a flickering pattern. An expanded view of such a flickering activity is shown above the upper trace

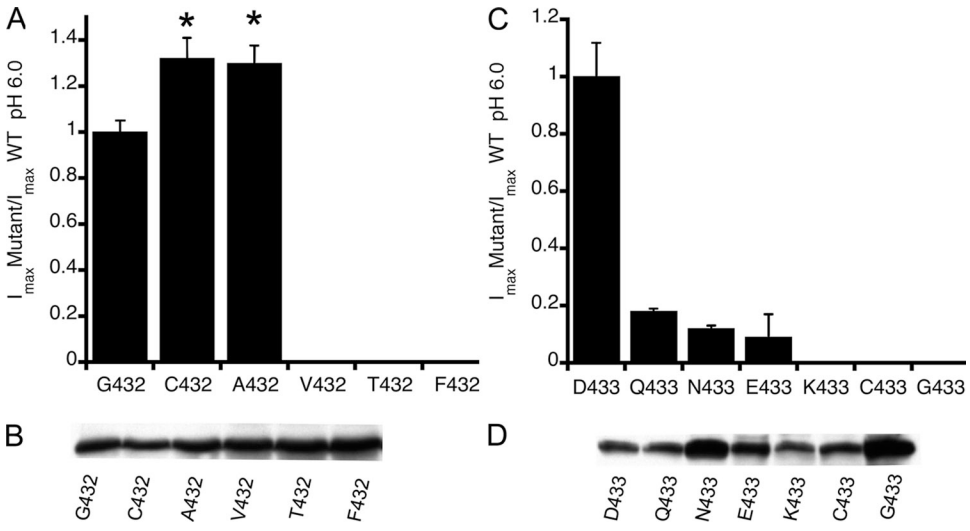

Figure 1. Relative magnitude of whole cell currents evoked by pH 6.0 of mutants in positions Gly-432 and Asp-433. (A) Normalized currents of Gly-432 substitutions. Columns are the average of ≥12 cells from three different preparations. Error bars are standard deviations. Asterisks indicate significant difference from G432 by unpaired *t* test, P ≤ 0.005. (B) Western blot of lASIC1 detected with anti-FLAG monoclonal antibody from eight oocytes injected with 5 ng cRNA that were biotinylated after measurements of whole cell currents by TEVC. (C) Normalized currents of substitutions of Asp-433. (D) Western blot of oocytes as shown in C, but oocytes expressing N433 and G433 were injected with 50 ng cRNA.

of D433Q (Fig. 3 D). The mean open time of the events within a burst was 2.2 ms. A histogram of the duration of open events of lASIC1-D433Q is shown in Fig. 3 E, where the line represents the fit with three exponential components. 25% of the opening events had a mean duration of 0.35 ms, 75% had a mean duration of 2 ms, and 5% had a mean open time of 95 ms.

Mutant D433N (Fig. 3 F) exhibits kinetics similar to those of D433Q (Fig. 3 D), whereas D433E (Fig. 3 G) resembles the parent channel: long uninterrupted openings were present, and no flickering activity was detected. A histogram of open event durations of D433E is also shown (Fig. 3 H), indicating that most events are longer than 10 ms, as in D433. However, Glu does not entirely mimic Asp, as indicated by the partial desensitization of the macroscopic currents.

The mutant G432C showed long openings similar to wild-type channels; the estimated mean open time of the long events was 1,380 versus 1,000 ms, and it was calculated from records containing fewer than four channels open simultaneously using the method described previously (Zhang et al., 2006) (Fig. 3 I). The estimate was used in place of histograms because of few patches expressing single channels and the low number of long events, despite their major contribution to the total current. The slightly increased mean open time likely explains the larger macroscopic current found in Fig. 1 A.

Collectively, these results show that Gln and Asn and to a lesser degree Glu in position 433 shorten the duration of the open conformation by inducing brief but frequent shut events. These residues allow the gate to close the pore, but because the closures are not stable, the channels reopen. This process repeated in succession gives rise to the flickering activity. Hydrophobic residues instead lead to nonfunctional channels likely because they stabilize the closing gate to such a degree that the channels remain shut. Substitution of Gly-432 by Cys had the opposite effect; namely, it lengthened the duration of the open state.

The negative charge of Asp-433 is not required for Ca^{2+} block of lASIC1

Ca^{2+} ions modify many properties of ASIC channels: Ca^{2+} competes with H^+ for binding in the extracellular domain, changing kinetics of activation and desensitization (Babini et al., 2002; Zhang et al., 2006). Ca^{2+} also blocks the ion pore from the extracellular side (de Weille and Bassilana, 2001; Zhang and Canessa, 2002; Immke and McCleskey, 2003), and there is some evidence that it may permeate some ASIC channels (Waldmann et al., 1997; Yermolaieva et al., 2004). Paukert et al. (2004) reported that the inhibition of macroscopic rat ASIC1a currents by Ca^{2+} could be abolished by the introduction of two mutations together: D432C and E425G, which correspond to Asp-433 and Glu-426 in lASIC1.

To explore whether Asp-433 is the site that binds Ca^{2+} and the role of the negative charge at the entrance of the pore, we examined the effect of Ca^{2+} in the amplitude of unitary currents of channels bearing either Asp or Gln in position 433. Outside-out patches containing few channels, with no more than two simultaneous openings, were activated by solutions of pH 7.0 supplemented with various concentrations of Ca^{2+} from nominal 0 to 6 mM. The pH of all activating solutions was kept constant at 7.0 to prevent changes in the ionization state of Asp-433 that could in turn change the affinity of the site for Ca^{2+} binding. As expected, when we increased the concentration of Ca^{2+}, we observed a reduction in the number of active channels as a result of the competition of Ca^{2+} for the H^+ activation sites in the extracellular domain; however, this effect did not interfere with measurements of unitary current amplitude,

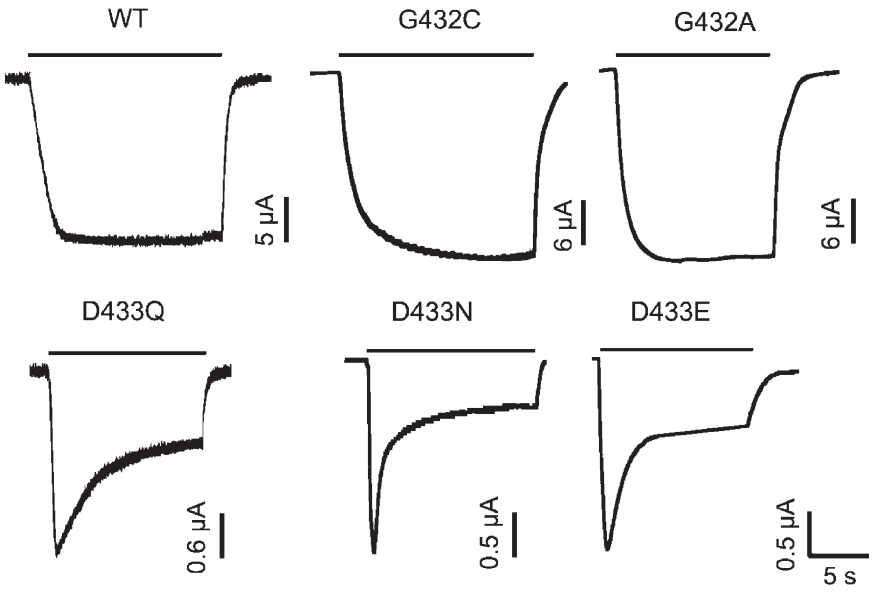

Figure 2. Macroscopic currents of Gly-432 and Asp-433 functional mutants. Representative examples of whole cell currents measured with TEVC. Wild-type channel encodes G432/D433. Substitutions of these positions are indicated for each example. Bars above traces mark the duration of pH 6.5 application. Baseline pH is 7.6. Membrane holding potential is −60 mV. Current and time scales are shown below each trace.

as long as enough channel activity remained in the patch. The protocol consisted in the application of the activating solution for 10 s, followed by recovery with a solution of pH 7.4 containing 1.5 mM Ca^{2+} applied for 2 s. Membrane voltage was changed in 20-mV steps from 20 to −100 mV. Sweeps were repeated up to 30 times in individual patches.

Fig. 4 A shows I-V curves of unitary currents of channels bearing Asp-433 in filled symbols and Qln-433 in open symbols. Current amplitude decreased as the concentration of Ca^{2+} increased with a slight voltage dependence visible as a decrease in conductance at very negative voltages. Fig. 4 B shows the voltage dependence of the $K_D(V)$ of Ca^{2+} block. The calculated K_D at 0 mV was 3.77 mM for Asp-433 and 3.98 mM for Gln-433. The fraction of the electric field traversed by a Ca^{2+} ion to reach the blocking site was estimated to be $\delta = 0.14$ according to Eq. 3.

The similar affinity for Ca^{2+} block of channels with Asp or Gln in position 433 suggests that the negative charge is not required for block or, alternatively, at pH 7.0 when Ca^{2+} binds to the open pore, the carboxylic group is most likely protonated.

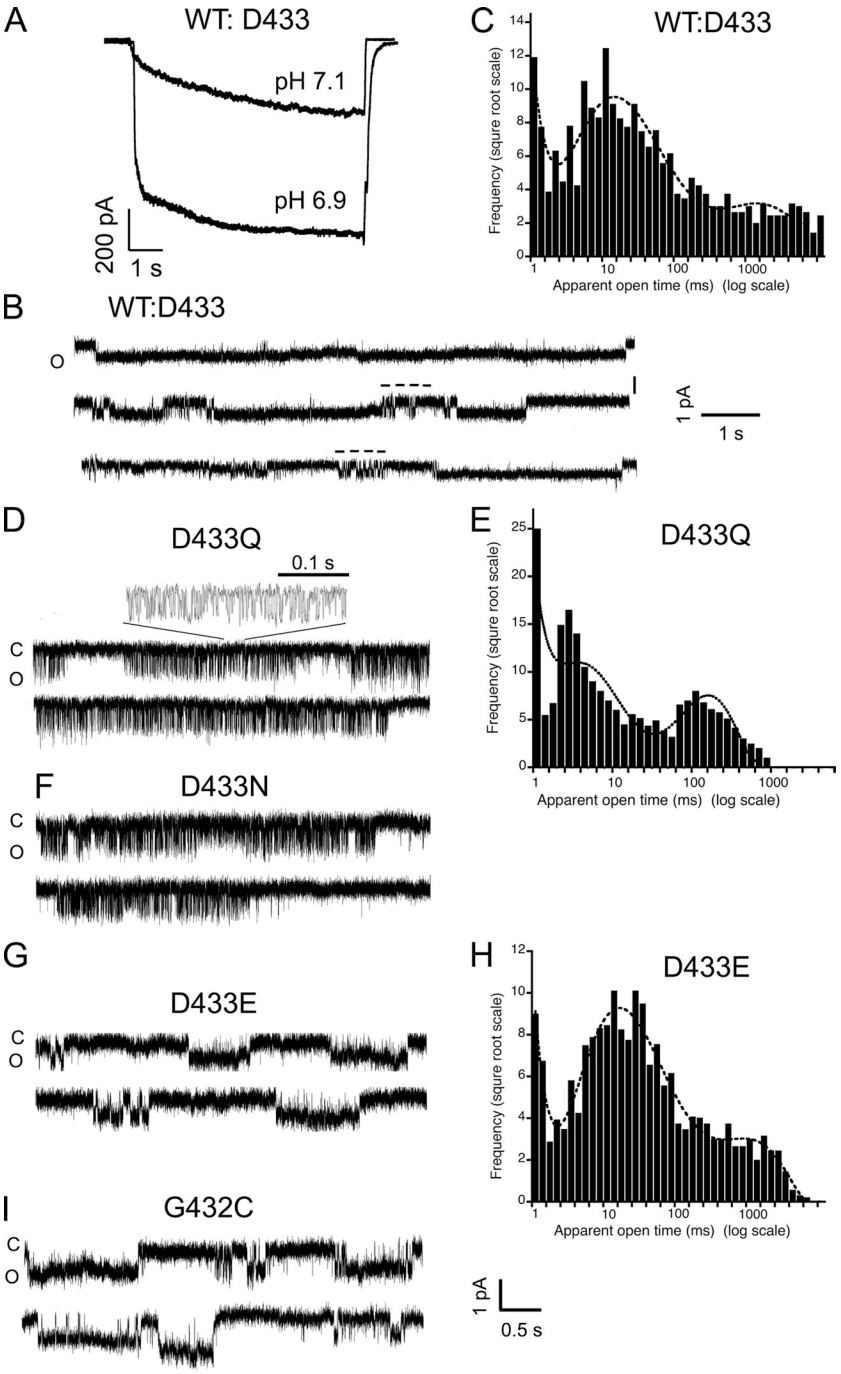

Figure 3. Kinetics of channels with substitutions in residues Asp-433 and Gly-432. (A) Currents from an outside-out patch expressing ~200 wild-type lASIC1 channels evoked by pH 7.1 and 6.9. (B) Single-channel events of wild-type lASIC1 show long openings of several-second duration and short openings indicated by stippled bars above the current trace. (C) Histogram of duration of open events fitted with three exponentials. (D) Single-channel activity of mutant D433Q. An expansion of the current is shown above the upper trace. (E) Histogram of duration of open events of ASIC1-D433Q. (F) Representative examples of single-channel activity from mutant D433N. (G) Single-channel recordings of D433E. (H) Histogram of duration of open events. (I) Unitary currents of G432C. C, closed state; O, open state. Amplitude and time scales indicated below traces. Holding potential is −60 mV for all examples.

Asp-433 does not determine ion selectivity or unitary conductance of lASIC1

The next issue explored was whether Asp-433 determines ion selectivity of lASIC1. We recorded I-V curves in the presence of Na^+, Li^+, K^+, or Cs^+ as the only cation in the external solution. For the mutants D433Q and D433N, the permeability ratios calculated from changes in reversal potential induced by each ion were P_{Li}/P_{Na}, 0.7 ± 0.1; P_K/P_{Na}, 0.28 ± 0.04; and P_{Cs}/P_{Na}, 0.037 ± 0.002 (Fig. 5 A). These ratios are not different from those of wild-type lASIC1 (Li et al., 2010). We also examined the relative permeability to Ca^{2+} by determining changes in reversal potential by external solutions containing exclusively 120 mM Na^+ or nominal 0 mM Ca^{2+}, or supplemented with 1.5, 3.0, or 6 mM Ca^{2+}. Fig. 5 B shows I-V curves of cells exposed sequentially to increasing external Ca^{2+} concentrations. Ca^{2+} does not displace the reversal potential obtained in the presence of only 120 mM Na^+ (35 mV) to more positive voltages, as expected if the channel is permeable to Ca^{2+}. However, external Ca^{2+} reduced the magnitude of the currents in a concentration-dependent manner, as in Fig. 5 A, because of block of the open pore. Fig. 5 C shows representative examples of channels bearing Asp-433 or Gln-433 recorded in 0 or 1.5 mM Ca^{2+}.

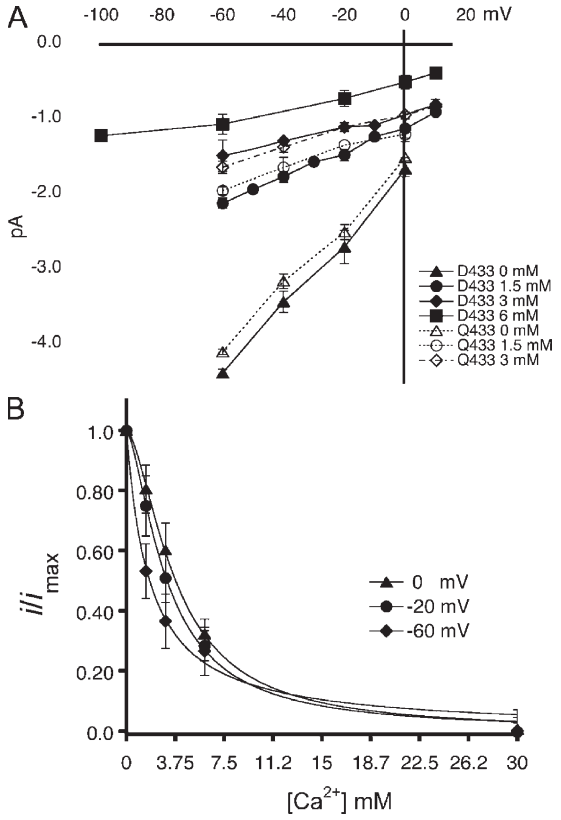

Figure 4. Ca^{2+} block of lASIC1 with Asp-433 or Gln-433. (A) I-V curves of unitary currents of lASIC1-Asp-433 (filled symbols) and lASIC-Gln-433 (open symbols) examined with various concentrations of Ca^{2+} in the external solution. All measurements were conducted at pH 7.0 to keep constant the ionization state of Asp-433. Composition of external solution (120 mM NaCl, 2 mM KCl, 15 mM HEPES, and Ca^{2+}) in the indicated concentrations. In 0 mM of solution, Ca^{2+} was not added to the solution: nominal zero. Each data point is the average of at least 10 independent measurements. Error bars are standard deviation. (B) Affinity of the Ca^{2+} site measured at various membrane voltages. The lines represent the fit of the data to Eq. 1. Values are K_D (0 mV), 3.7 mM and $n = 1.3$; K_D (−20 mV), 3.11 mM and $n = 1.2$; and K_D (−60 mV), 1.78 and $n = 1$.

The unitary conductance measured with 120 mM Na^+ outside and 120 K^+ in the pipette solution of outside-out patches and in the voltage range of −60 to 0 mV was 45 ± 4 and 41 ± 3 pS for wild type and D433Q in the absence of Ca^{2+}. The conductance was reduced to 18 ± 2 and 16 ± 2 pS in 1.5 mM Ca^{2+} for wild type and D433Q. Therefore, despite its location in the narrowest point of the conduction pathway, Asp-433 does not determine ion selectivity or unitary conductance, implying that the conformation of TM2 in the open state differs substantially from that in the closed state provided by the atomic structure of cASIC1 (Gonzales et al., 2009).

Mutations of Gly-432 or Asp-433 change the apparent proton affinity for channel activation

As we mentioned above, substitutions of Gly-432 by larger residues in the mammalian ASIC2a facilitate openings by increasing the apparent proton affinity for channel activation. Here, we observed that the mutant G432C in lASIC1 also displaced the pH_{50A} toward more alkaline pH, from 7.0 to 7.2, although the shift was modest, as lASIC1 channels already exhibit high proton affinity (Fig. 6). On the other hand, the substitution D433Q shifted the affinity to the acidic range, pH_{50A} 6.8. Of note, the Hill coefficients, indicators of intersubunit cooperativity to open the pore, changed in the same direction as the pH_{50A}: from $n = 6$ in G432C to $n = 2$ in D433Q. These results show that modification of the desensitization gate leads to changes in both activation and desensitization, as if the gates for these two processes are in close proximity or functionally coupled.

DISCUSSION

One of the main findings of this work is that substitutions of Asp-433 markedly shorten the duration of the open state of lASIC1 by inducing frequent and short shut events: Asp-433 keeps long opening, whereas Gln and Asn reduce the duration of open events, and hydrophobic residues abolish currents in lASIC1. Thus, residue 433 blocks ion flow through the pore, with various degrees of efficiency depending of the nature of the side chain. Assuming that the shut events represent closures of the pore, the previous observations together with Asp-433 location in the narrowest segment of the ion pathway when the channel is in a nonconducting conformation (crystal structure) agree with the notion

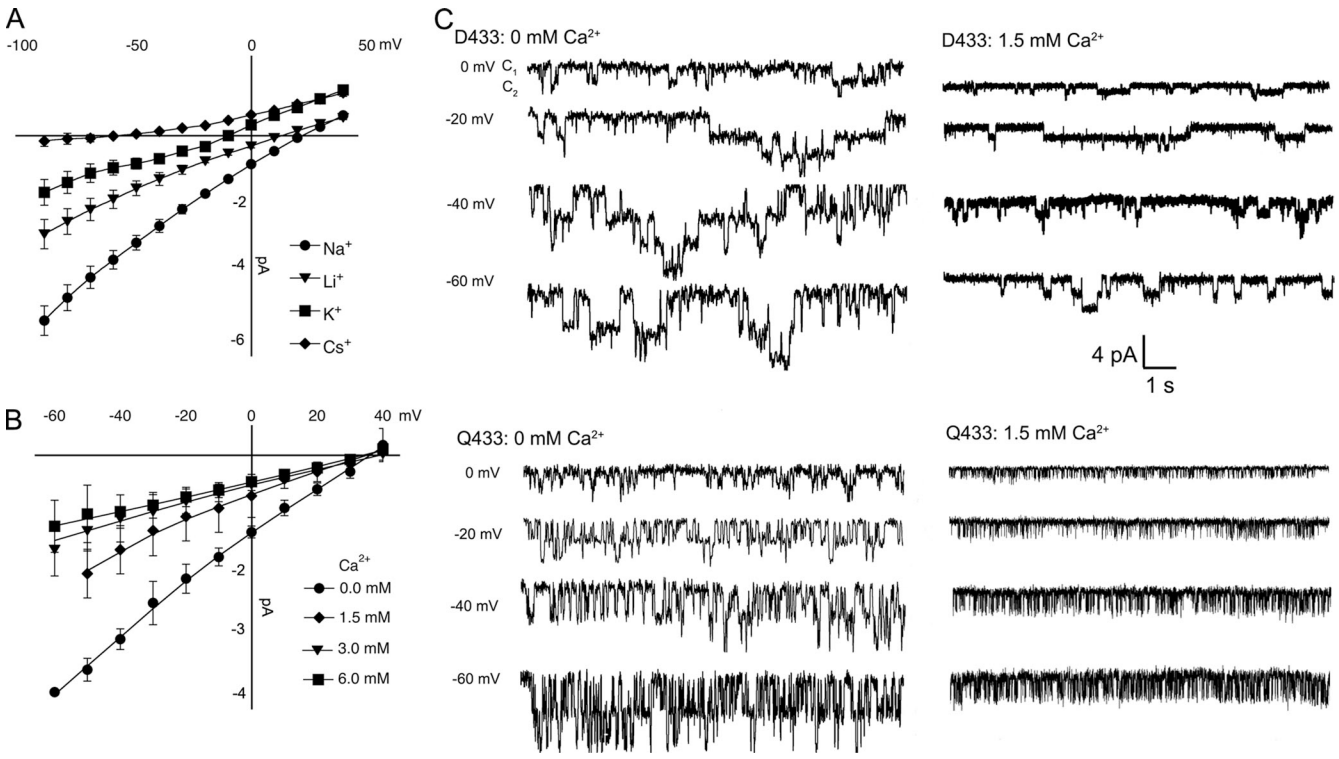

Figure 5. Substitution of Asp-433 for Gln maintains the same ion selectivity. (A) I-V curves of lASIC1-D433Q in the presence of external solutions containing 120 mM Na^+, Li^+, K^+, or Cs^+ without Ca^{2+}. (B) I-V curves of lASIC1-D433Q in the presence of 120 mM Na^+ alone or supplemented with the indicated amounts of Ca^{2+}. Data points are the mean ± SD of five independent measurements. Permeability ratios of monovalent cations were calculated by changes in reversal potential according to Eq. 2. (C) Representative examples of unitary currents of channels bearing Asp-433 or Gln-433 in 0 or 1.5 mM Ca^{2+} in the activating solution (pH 7.0 recorded at the indicated voltages). Amplitude and time scale are the same for all traces.

that Asp-433 forms the "closing gate." The term "gate" has been traditionally used in voltage-sensitive K^+ and Na^+ channels to name the domain of the protein that blocks the passage of ions, without reference to its nature or location in the channel: it can be a constriction of the pore or an intracellular or extracellular element that swings into the ion pathway, occluding access of ions to the pore. In ASIC1, the closing gate is embedded in the outer part of the TM2 α helix and appears to operate as a constriction of the lumen.

We also observed that substitutions of Asp-433 induced partial desensitization to lASIC1. Here, desensitization is understood as the long-lasting closure of all or a fraction of channels in the continual presence of external H^+. What could be the relation of the closing gate and desensitization? First, it is evident that although all ASICs share Asp-433, the extent and kinetics of desensitization vary among channels. Second, other elements in the channel protein located in TM1 and the extracellular domain modify desensitization. Specifically, residue Trp-64 in the outer segment of TM1 and adjacent to the desensitization gate markedly decreases the mean open time and speeds desensitization kinetics of lASIC1 (Li et al., 2010). Similarly, substitutions of the outer segment of TM1 have been shown to alter desensitization kinetics of rat ASIC3 (Salinas et al., 2009). On the other hand, mutations and modifications of residues located in the extracellular domain also change the speed and extent of desensitization in rat ASIC3 (Cushman et al., 2007).

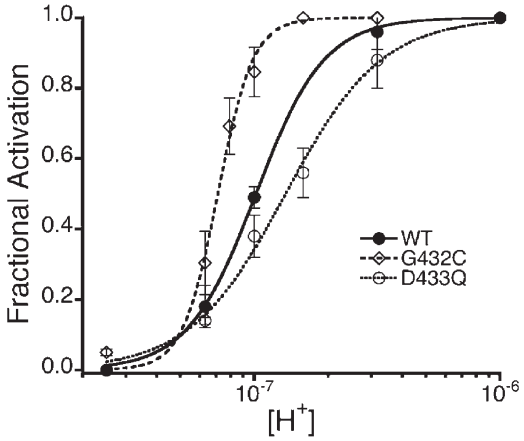

Figure 6. Apparent affinity of protons for the activation of mutants G432C and D433Q. Dose–response curves of proton activation of mutants G432C and D433Q compared with the parent channel. Lines are fits of the data to Eq. 1. Values of the half-maximal proton concentration for activation or pH_{50A} were 7.2, 7.0, and 6.8, and $n = 6$, $n = 3$, and $n = 2$ for G432C, wild type (WT), and D433Q, respectively.

Thus, we conceive the highly conserved Asp-433 in the closing gate as the element that forms the lock and determines the efficiency of closures, whereas the extent and kinetics of desensitization are determined by other less conserved domains in the channel protein that control the on and off position of the gate, most likely by positioning TM2, which contains the closing gate.

Although mutations of Asp-433 make the closing gate more efficient, mutations of the adjacent residue Gly-432 by Cys or Ala decrease frequency of shut events, i.e., make the gate less efficient, thereby lengthening the open events. An observation that has been reproduced in our laboratory and also by other groups (Waldmann et al., 1997) is that substitutions of Gly-432 in rat, frog, fish, and chicken ASIC1 by residues with large side chains eliminate current rather than remove desensitization and/or increase the pH_{50A}, as in ASIC2a (Waldmann et al., 1996; Champigny et al., 1998) and in the degenerins (Hong and Driscoll, 1994; Huang and Chalfie, 1994). In lASIC1, only small side chains in 432 increased the mean duration of open events and the pH_{50A}, whereas large side changes abolished currents. This lends additional support to the notion that minor differences in the architecture of the outer pore result in significant changes in channel gating and kinetics.

Our interpretation of the data implies that underlying the frequent shut events are intermittent closures produced by constriction of the gate. However, in the strictest sense, we cannot equate with certainty shut events defined by electrophysiological measurements to physical occlusion of the pore by the closing gate. It is plausible, although unlikely, that another structure near or around the pore senses replacements of Asp-433 or Gly-432, leading to obstruction of ion flow by other means.

The other significant finding in this study is that Asp-433 does not determine ion selectivity, despite the side chain of this residue pointing to the lumen, occluding the pore, and coordinating a Cs^+ ion in the crystal structure of cASIC1. Substitutions by Gln or Asn neither changed the selectivity sequence of permeant cations $Na^+ > Li^+ > K^+ >> Cs^+$ nor the unitary conductance. These results imply that the side chain of Asp-433 most likely is neutral in the open state because of protonation or, if negatively charged, because it is away from the lumen so as not to interfere with the passage of ions through the permeation pathway. The results from examining Ca^{2+} block agree with Asp-433 being protonated when the channel is in the open state, pH 7.0, because substitution by the neutral residue Gln did not change the values of the K_D or the voltage dependence of Ca^{2+} block. Another possibility is that Asp-433 is not the Ca^{2+}-binding site; thus, substitution by Gln produces little effect on the affinity and voltage dependence of block. Indeed, the voltage dependence of block places the Ca^{2+}-binding site close to amiloride binding, which is Ser-583 in αENaC (Schild et al., 1997) and has a δ of ~0.15 (McNicholas and Canessa, 1997; Fyfe and Canessa, 1998), similar to Ca^{2+}. The Ser-583 in αENaC corresponds to Gly-439 in ASIC1; hence, Ca^{2+} may enter the pore as deep as amiloride but cannot pass through the narrow selectivity filter.

In summary, we show that residues in positions 432 and 433 determine the duration of the open state by virtue of controlling the efficiency of the closing gate to constrict the pore, but they do not participate in defining ion selectivity, conductance of permeant ions, or fast block of the open pore by Ca^{2+}. Collectively, these results imply that the closing gate and selectivity filter are distinct structures in the pore. The second observation is that changes in activation and desensitization occur together and in the same direction, as if the putative "activation" and "closing" gates of ASIC1 were the same physical entity and/or functionally coupled.

Lawrence G. Palmer served as editor.

Submitted: 18 November 2010
Accepted: 9 February 2011

REFERENCES

Babini, E., M. Paukert, H.S. Geisler, and S. Grunder. 2002. Alternative splicing and interaction with di- and polyvalent cations control the dynamic range of acid-sensing ion channel 1 (ASIC1). *J. Biol. Chem.* 277:41597–41603. doi:10.1074/jbc.M205877200

Chalfie, M., and E. Wolinsky. 1990. The identification and suppression of inherited neurodegeneration in Caenorhabditis elegans. *Nature.* 345:410–416. doi:10.1038/345410a0

Champigny, G., N. Voilley, R. Waldmann, and M. Lazdunski. 1998. Mutations causing neurodegeneration in Caenorhabditis elegans drastically alter the pH sensitivity and inactivation of the mammalian H^+-gated Na^+ channel MDEG1. *J. Biol. Chem.* 273:15418–15422. doi:10.1074/jbc.273.25.15418

Cushman, K.A., J. Marsh-Haffner, J.P. Adelman, and E.W. McCleskey. 2007. A conformation change in the extracellular domain that accompanies desensitization of acid-sensing ion channel (ASIC) 3. *J. Gen. Physiol.* 129:345–350. doi:10.1085/jgp.200709757

de Weille, J., and F. Bassilana. 2001. Dependence of the acid-sensitive ion channel, ASIC1a, on extracellular Ca^{2+} ions. *Brain Res.* 900:277–281. doi:10.1016/S0006-8993(01)02345-9

Driscoll, M., and M. Chalfie. 1991. The mec-4 gene is a member of a family of Caenorhabditis elegans genes that can mutate to induce neuronal degeneration. *Nature.* 349:588–593. doi:10.1038/349588a0

Fyfe, G.K., and C.M. Canessa. 1998. Subunit composition determines the single channel kinetics of the epithelial sodium channel. *J. Gen. Physiol.* 112:423–432. doi:10.1085/jgp.112.4.423

Gonzales, E.B., T. Kawate, and E. Gouaux. 2009. Pore architecture and ion sites in acid-sensing ion channels and P2X receptors. *Nature.* 460:599–604. doi:10.1038/nature08218

Hille, B. 1992. Ionic Channels in Excitable Membranes. 2nd ed. Sinauer Associates, Inc., Sunderland, MA. 607 pp.

Hong, K., and M.A. Driscoll. 1994. A transmembrane domain of the putative channel subunit MEC-4 influences mechanotransduction and neurodegeneration in *C. elegans*. *Nature.* 367:470–473. doi:10.1038/367470a0

Huang, M., and M. Chalfie. 1994. Gene interactions affecting mechanosensory transduction in Caenorhabditis elegans. *Nature.* 367:467–470. doi:10.1038/367467a0

Immke, D.C., and E.W. McCleskey. 2003. Protons open acid-sensing ion channels by catalyzing relief of Ca^{2+} blockade. *Neuron.* 37:75–84. doi:10.1016/S0896-6273(02)01130-3

Li, T., Y. Yang, and C.M. Canessa. 2010. Two residues in the extracellular domain convert a nonfunctional ASIC1 into a proton-activated channel. *Am. J. Physiol. Cell Physiol.* 299:C66–C73. doi:10.1152/ajpcell.00100.2010

McNicholas, C.M., and C.M. Canessa. 1997. Diversity of channels generated by different combinations of epithelial sodium channel subunits. *J. Gen. Physiol.* 109:681–692. doi:10.1085/jgp.109.6.681

Paukert, M., E. Babini, M. Pusch, and S. Gründer. 2004. Identification of the Ca^{2+} blocking site of acid-sensing ion channel (ASIC) 1: implications for channel gating. *J. Gen. Physiol.* 124:383–394. doi:10.1085/jgp.200308973

Salinas, M., M. Lazdunski, and E. Lingueglia. 2009. Structural elements for the generation of sustained currents by the acid pain sensor ASIC3. *J. Biol. Chem.* 284:31851–31859. doi:10.1074/jbc.M109.043984

Schild, L., E. Schneeberger, I. Gautschi, and D. Firsov. 1997. Identification of amino acid residues in the α, β, and γ subunits of the epithelial sodium channel (ENaC) involved in amiloride block and ion permeation. *J. Gen. Physiol.* 109:15–26. doi:10.1085/jgp.109.1.15

Waldmann, R., G. Champigny, N. Voilley, I. Lauritzen, and M. Lazdunski. 1996. The mammalian degenerin MDEG, an amiloride-sensitive cation channel activated by mutations causing neurodegeneration in Caenorhabditis elegans. *J. Biol. Chem.* 271:10433–10436. doi:10.1074/jbc.271.18.10433

Waldmann, R., G. Champigny, F. Bassilana, C. Heurteaux, and M. Lazdunski. 1997. A proton-gated cation channel involved in acid-sensing. *Nature.* 386:173–177. doi:10.1038/386173a0

Woodhull, A.M. 1973. Ionic blockage of sodium channels in nerve. *J. Gen. Physiol.* 61:687–708. doi:10.1085/jgp.61.6.687

Yermolaieva, O., A.S. Leonard, M.K. Schnizler, F.M. Abboud, and M.J. Welsh. 2004. Extracellular acidosis increases neuronal cell calcium by activating acid-sensing ion channel 1a. *Proc. Natl. Acad. Sci. USA.* 101:6752–6757. doi:10.1073/pnas.0308636100

Zhang, P., and C.M. Canessa. 2002. Single channel properties of rat acid–sensitive ion channel-1α, -2a, and -3 expressed in *Xenopus oocytes. J. Gen. Physiol.* 120:553–566. doi:10.1085/jgp.20028574

Zhang, P., F.J. Sigworth, and C.M. Canessa. 2006. Gating of acid-sensitive ion channel-1: release of Ca^{2+} block vs. allosteric mechanism. *J. Gen. Physiol.* 127:109–117. doi:10.1085/jgp.200509396